A COMPARISON BETWEEN TIME DOMAIN AND FREQUENCY DOMAIN CALCULATIONS OF STATIONARY NEUTRON FLUCTUATIONS

M. Viebach[1], C. Lange[1], S. Kliem[2], C. Demazière[3], U. Rohde[4], D. Hennig[1], and A. Hurtado[1]

[1]Technische Universität Dresden, Chair of Hydrogen and Nuclear Energy
George-Bähr-Straße 3b, D-01069 Dresden, Germany

[2]Helmholtz-Zentrum Dresden-Rossendorf, Reactor Safety Division
Bautzner Landstraße 400, D-01328 Dresden, Germany

[3]Chalmers University of Technology, Department of Physics,
Divivion of Subatomic and Plasma Physics, SE-412 96 Gothenburg, Sweden

[4]HZDR-Innovation Rossendorf
Bautzner Landstraße 400, D-01328 Dresden, Germany

marco.viebach@tu-dresden.de, s.kliem@hzdr.de, demaz@chalmers.se

ABSTRACT

Unexplained neutron flux fluctuation patterns observed in some reactors were recently investigated by various European institutions. The time-domain code *DYN3D* is one of the tools used for simulating these fluctuations. Though, the applicability of time-domain codes for modelling small stationary fluctuations remains a discussed question.

Aiming at a confirmation that these codes may be applied for neutron noise calculations, two special cases of neutron flux oscillations have been simulated with *DYN3D* and with *CORE SIM*, the latter one being validated for the context here. The comparison between the results of these two codes is the subject of this paper.

This study demonstrates that time- and frequency-dependent calculations can give qualitatively equivalent results but substantial quantitative deviations may occur. Nevertheless, *DYN3D* may be considered as qualified for neutron-noise calculations as the deviations are smaller than 20 %. The optimization of the *DYN3D* setup is a matter of future research.

KEYWORDS: neutron noise, DYN3D, CORE SIM

1. INTRODUCTION

For roughly two decades, stationary neutron flux fluctuations have received increased attention (cf. [1]), as their amplitudes have exhibited insufficiently interpreted cycle-by-cycle increases or decreases in numerous pressurized water reactors. The topic has become relevant especially with KWU (Kraftwerk Union) built reactors [2]. Here, the power limitation system is sensitive to (high) neutron flux fluctuation amplitudes, performing an automatic power reduction if given criteria are met.

In order to better understand their general phenomenology, neutron flux fluctuations have been simulated with dedicated tools such as *CORE SIM* [3] (e. g. [4]) and also by transient codes such as *DYN3D* [5,6] (e. g. [7]). The applicability of the latter codes for such purposes, which is not ad hoc clear, was recently investigated (see e. g. [8] and also [9]). In this context, a comparison between *CORE SIM* and *DYN3D* is the matter of the present contribution.

As for *CORE SIM* validation cases exist, the comparison explicitly aims on providing a first step of a validation of *DYN3D* neutron-flux-fluctuation simulations. Thus, the paper at hand can be used to improve the interpretability of *DYN3D* neutron noise calculations. It has to be emphasized that its focus is not testing the validity of diffusion theory [*], which is the foundation of both codes, but probing the applicability of time-domain codes in the given context.

The two applied codes provide complementary approaches for covering the dynamics, i. e. *DYN3D* solves the diffusion equations in the time domain (cf. [5,6]) and *CORE SIM* solves them in the frequency domain (cf. [3]). For the comparison, selected sinusoidal perturbations are applied at fixed frequencies and the induced neutron flux fluctuations are considered in terms of the spatial distributions of their amplitude and their phase. It should be noted that perfect agreement of the results is not expected for the time being. Note that a comparison of *PARCS* and *CORE SIM* calculations resulted in deviations of more than $10\,\%$ in some occurences (cf. [8]).

2. COMPARISON BETWEEN TIME AND FREQUENCY DOMAIN CALCULATIONS

2.1. Models and Methods

2.1.1. Used codes

The used version of the code *DYN3D* solves the (non-linearized) two-group diffusion equation in the time domain using nodal methods for the spatial dependence and taking into account six groups of delayed neutron precursors. The used version of the code *CORE SIM* solves the linearized [†] two-group diffusion equation in the frequency domain using finite-differences methods for the spatial dependence and taking into account one group of delayed neutron precursors.

The used reactor model corresponds to the OECD/NEA and U.S. NRC PWR MOX/UO2 Core Transient Benchmark [11]. See Fig. 1 for the spatial layout. All simulations presented here are based on the corresponding *DYN3D* input [‡]. The wide-range two-group macroscopic cross-section library was generated using the lattice code *HELIOS* [13]. In *HELIOS*, each fuel assembly type present in the core is modelled with all details in 2D. The obtained data are condensed to two groups and tabulated against burn-up and feedback parameters.

The calculation procedure is as follows. First, a steady-state *DYN3D* run is performed. On the one hand, its solution is the starting point for the time-dependent *DYN3D* run. On the other hand, the distribution of cross section data (XS), converged w. r. t. thermal hydraulics, is used to define the *CORE SIM* material data input. The kinetics *CORE SIM* input (β_{eff}, λ, v_1, and v_2) is derived from

[*] For a comparison of *CORE SIM* with a solver employing transport theory, Ref. [10] may be consulted.

[†] Application of linearization, i. e. neglection higher-order terms, is justified as only small perturbations are considered here.

[‡] The *DYN3D* input was prepared in the context of solving the nodal multigroup SP_3 equations with *DYN3D* for the OECD/NEA and U.S. NRC PWR MOX/UO2 Core Transient Benchmark exercise (cf. [12]).

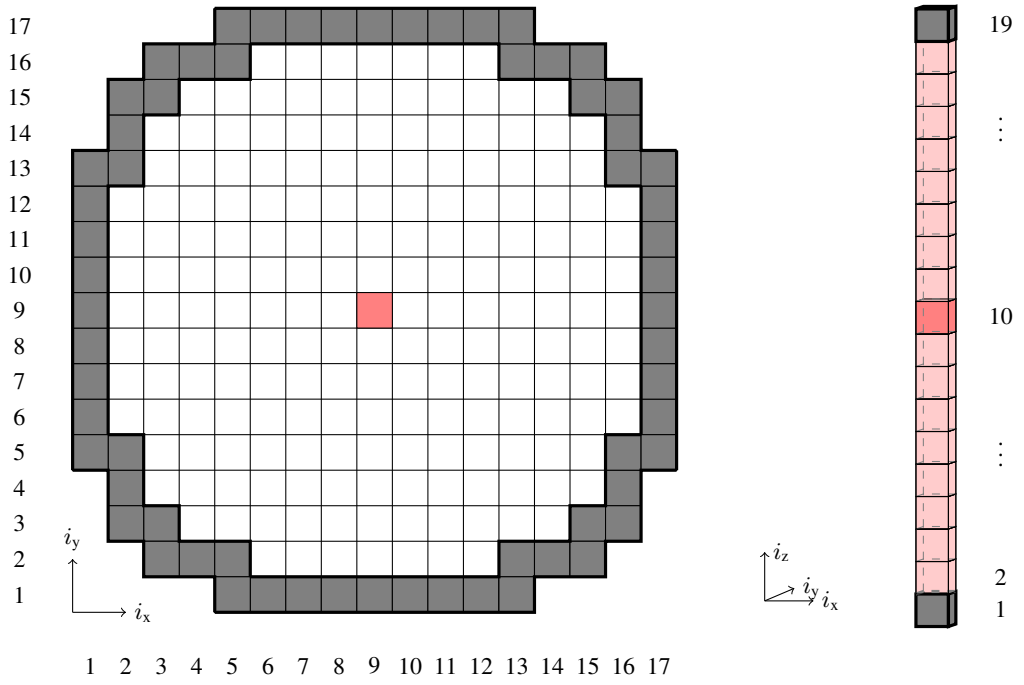

(a) Radial-azimuthal (b) Axial

Figure 1: Layout of the reactor for both *DYN3D* and *CORE SIM* calculations. For the latter, the spatial grid is refined by factor 2 in each dimension. Reflector areas are represented in gray. Regions considered for the perturbations are represented in shades of red.

the corresponding *DYN3D* output, as well. Taking the given material data, *CORE SIM* performs its own steady-state run, which initializes the subsequent calculation of the neutron flux fluctuations in the frequency domain. The *CORE SIM* calculations are performed with a spatial grid refined by factor 2 w. r. t. the nodal dimensions of the *DYN3D* calculations (i. e. each node is divided into 8 equally sized subregions).

In order to provide similar conditions for both types of calculations, some *DYN3D* settings and source-code details were adapted to match with the *CORE SIM* model: vacuum boundary conditions, no assembly discontinuity factors (ADFs), no feedback (in the transient calculation), manipulation of selected cross section values of selected nodes. The time-dependent neutron flux distributions (fast and thermal) are written to file. The fission source iteration accuracy was increased from $\epsilon_\mathrm{f} = 10^{-5}$ ("recommended value") to $\epsilon_\mathrm{f} = 10^{-10}$.

2.1.2. Perturbation of the system

The codes are used to calculate neutron noise in the time domain $(\delta\phi_1(i_\mathrm{x}, i_\mathrm{y}, i_\mathrm{z}, t), \delta\phi_2(i_\mathrm{x}, i_\mathrm{y}, i_\mathrm{z}, t))$ and in the frequency domain $(\widetilde{\delta\phi}_1(i_\mathrm{x}, i_\mathrm{y}, i_\mathrm{z}, f), \widetilde{\delta\phi}_2(i_\mathrm{x}, i_\mathrm{y}, i_\mathrm{z}, f))$. For the sake of simplicity, only the thermal absorption cross section $\Sigma_{\mathrm{abs},2}$ was modified:

$$\begin{aligned} \Sigma_{\mathrm{abs},2}(i_\mathrm{x}, i_\mathrm{y}, i_\mathrm{z}, t) &= \Sigma_{\mathrm{abs},2,0}(i_\mathrm{x}, i_\mathrm{y}, i_\mathrm{z}) + \delta\Sigma_{\mathrm{abs},2}(i_\mathrm{x}, i_\mathrm{y}, i_\mathrm{z}, t) \\ &= \Sigma_{\mathrm{abs},2,0}(i_\mathrm{x}, i_\mathrm{y}, i_\mathrm{z}) + A(i_\mathrm{x}, i_\mathrm{y}, i_\mathrm{z}) \cdot \sin(2\pi f' t + \alpha(i_\mathrm{x}, i_\mathrm{y}, i_\mathrm{z})) \end{aligned} \quad (1)$$

with $\Sigma_{\text{abs,2,0}}$ being the steady-state value of the cross section, i_x, i_y, i_z being the spatial node indices, $\delta\Sigma_{\text{abs,2}}$ being the time dependent perturbation, A being the amplitude, f' being the frequency, and α being the phase. The transformation of the perturbation to the frequency domain gives

$$\widetilde{\delta\Sigma}_{\text{abs,2}}(i_\text{x}, i_\text{y}, i_\text{z}, f) \;=\; A(i_\text{x}, i_\text{y}, i_\text{z}) \cdot \frac{i}{2}\left[\delta(f-f')e^{-i\alpha(i_\text{x},i_\text{y},i_\text{z})} - \delta(f+f')e^{i\alpha(i_\text{x},i_\text{y},i_\text{z})}\right]. \tag{2}$$

The amplitude is expressed in terms of a relative amplitude A_{rel},

$$A(i_\text{x}, i_\text{y}, i_\text{z}) = A_{\text{rel}} \cdot \Sigma_{\text{abs,2,0}}(i_\text{x}, i_\text{y}, i_\text{z}). \tag{3}$$

2.1.3. Considered perturbation cases

a) **Absorber of variable strength at fixed location**

$$A(i_\text{x}, i_\text{y}, i_\text{z}) \;=\; \begin{cases} A_{\text{rel}} \cdot \Sigma_{\text{abs,2,0}}(i_\text{x}, i_\text{y}, i_\text{z}), & \text{for } i_\text{x}=9, i_\text{y}=9, i_\text{z}=10 \\ 0, & \text{else} \end{cases} \tag{4}$$

$$\alpha(i_\text{x}, i_\text{y}, i_\text{z}) \;=\; 0\,. \tag{5}$$

b) **Absorber of variable strength travelling from bottom to top**
At time $t = t'$, the perturbation of a node in the lowermost location, $i_\text{z} = 1$,

$$\delta\Sigma_{\text{abs,2}}(i_\text{x}, i_\text{y}, 1, t') = A(i_\text{x}, i_\text{y}, 1) \cdot \sin(2\pi f' t' + \alpha(i_\text{x}, i_\text{y}, 1)) \tag{6}$$

is ahead of the perturbation of the nodes above, $i_\text{z} = 2, \ldots, 19$, by $\Delta t_{i_\text{z}} = \Delta t(i_\text{z}) - \Delta t(1)$. Therefore,

$$\delta\Sigma_{\text{abs,2}}(i_\text{x}, i_\text{y}, i_\text{z}, t') = A(i_\text{x}, i_\text{y}, i_\text{z}) \cdot \sin(2\pi f'(t' - \Delta t_{i_\text{z}}) + \alpha(i_\text{x}, i_\text{y}, 1)). \tag{7}$$

Assuming a perturbation travelling velocity v and an equal distance Δz between the center of axially adjacent nodes, the time shift at layer i_z relative to the virtual layer $i_\text{z} = 0$ reads as

$$\Delta t(i_\text{z}) = \frac{\Delta z}{v} i_\text{z}. \tag{8}$$

And after specifying the perturbation frequency f' and setting the phase of the virtual layer $i_\text{z} = 0$ to $\alpha(i_\text{x}, i_\text{y}, 0) = 0$, the axial layers' time shifts can be expressed by the perturbation phases as

$$\alpha(i_\text{x}, i_\text{y}, i_\text{z}) = -2\pi f' \frac{\Delta z}{v} i_\text{z}. \tag{9}$$

Thus, a perturbation travelling vertically up in the central channel is described here by

$$\begin{aligned} A(i_\text{x}, i_\text{y}, i_\text{z}) \;&=\; \begin{cases} A_{\text{rel}} \cdot \Sigma_{\text{abs,2,0}}(i_\text{x}, i_\text{y}, i_\text{z}), & \text{for } i_\text{x}=9, i_\text{y}=9, i_\text{z}=2,\ldots 18 \\ 0, & \text{else,} \end{cases} \\ \alpha(i_\text{x}, i_\text{y}, i_\text{z}) \;&=\; \begin{cases} -2\pi f' \frac{\Delta z}{v} i_\text{z}, & \text{for } i_\text{x}=9, i_\text{y}=9, i_\text{z}=2,\ldots 18 \\ 0, & \text{else}\,. \end{cases} \end{aligned} \tag{10}$$

The nodes of the axial reflectors are excluded from the explicit perturbation.

2.1.4. Extraction of the results

The results were prepared to compare amplitudes and phases. For the frequency domain, the fluctuations $(\widetilde{\delta\phi}_1, \widetilde{\delta\phi}_2)$ are directly available through the *CORE SIM* output, i. e. absolute value and phase of complex numbers. The distribution of absolute values was normalized to the steady-state distributions $(\phi_{1,0}, \phi_{2,0})$ to provide the distribution of relative fluctuation amplitudes. In order to provide a spatial resolution compatible with that of *DYN3D*, the results were coarsened by averaging the subregion solutions over the initial node regions.

For the time domain, evaluation of amplitudes and phases was performed via the following procedure. After the steady-state calculation, the transient calculation was performed with a temporal length of $10.1\,\mathrm{s}$ and a neutron-kinetics time step of $\Delta t_{\mathrm{NK}} = 10^{-3}\,\mathrm{s}$. The perturbation was updated with a time step of $\Delta t_{\mathrm{TH}} = 10^{-2}\,\mathrm{s}$. Only the last lapse of time that covers an entire perturbation period (e. g. 9.0 - $10.0\,\mathrm{s}$ for perturbations with $f' = 1\,\mathrm{Hz}$) was analyzed. For each considered location (node), the fluctuation was obtained by subtracting from the flux values its mean value. The fluctuations were normalized to this mean value afterwards. For the resulting relative fluctuation, the amplitude was calculated as $(\max(\delta\phi_{1/2}/\phi_{1/2,0}) - \min(\delta\phi_{1/2}/\phi_{1/2,0}))/2$. The phase was evaluated by determining the time shift between the minima of the functions $\delta\phi_{1/2}/\phi_{1/2,0}$ and the minima of the oscillating perturbation. The location of the minima of $\delta\phi_{1/2}/\phi_{1/2,0}$ was determined by interpolating the fluctuation time points with cubic splines (using scipy.interpolate.interp1d in *PYTHON*) and finding the minima of the interpolation (using scipy.optimize.fminbound in *PYTHON*).

Note that two different relative units are defined: fluctuation amplitude relative to the mean value of the neutron flux in $\%_{\mathrm{s}}$, and deviation of the *DYN3D* solution's amplitudes relative to the corresponding *CORE SIM* solution's amplitudes in $\%_{\mathrm{a}}$.

2.2. Results

2.2.1. Steady-state solutions

Figure 2 compares the steady-state solutions for both types of simulations. Regarding k_{eff}, the solutions differ by $-19.7\,\mathrm{pcm}$, and from visual inspection, no qualitative difference can be seen. The consulted (pointwise) quadratic relative deviation $\mathrm{qdev}_{1/2} = (\phi_{\textit{DYN3D},1/2,0} - \phi_{\textit{CORE SIM},1/2,0})^2/\phi^2_{\textit{CORE SIM},1/2,0}$ takes core-wide average values of $2.2\,\%$ for the fast group and $1.0\,\%$ for the thermal group. Therefore, the two models are considered as comparable to one another at first w. r. t. the steady-state solutions. This is required for comparing the time-dependent solutions.

2.2.2. Absorber of variable strength at fixed location

Figure 3 shows the neutron flux fluctuations induced by an absorber of sinusoidal strength located at the center of the reactor core. Both simulations, with *DYN3D* and with *CORE SIM*, give qualitatively equivalent results. The maximum induced fluctuation amplitude is found at the perturbation's location and is in the range of percents; the larger the distance from the perturbation, the smaller the fluctuation amplitude is; the phase is close to π at the perturbation's location and slightly increases for moving away from the perturbation.

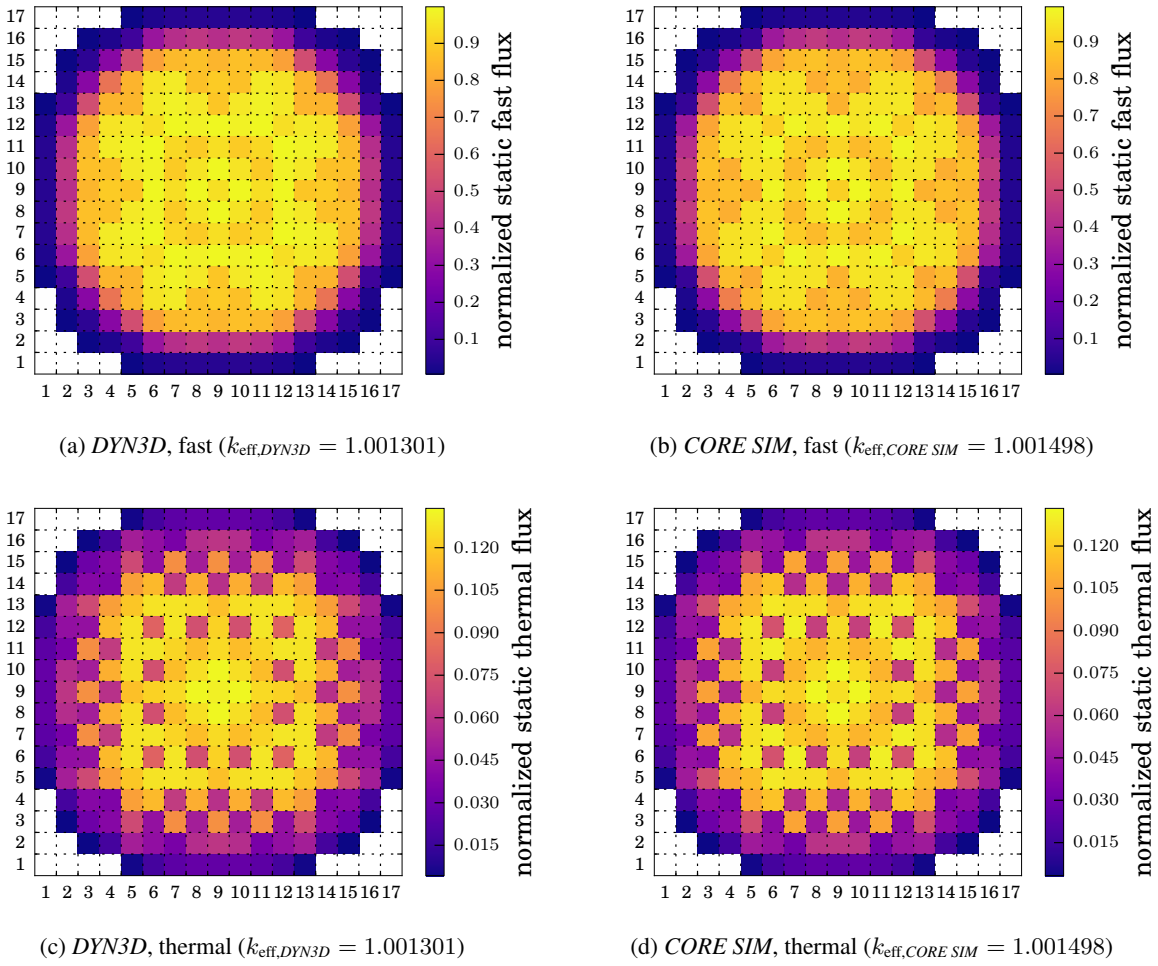

(a) *DYN3D*, fast ($k_{\text{eff},DYN3D} = 1.001301$)

(b) *CORE SIM*, fast ($k_{\text{eff},CORE\ SIM} = 1.001498$)

(c) *DYN3D*, thermal ($k_{\text{eff},DYN3D} = 1.001301$)

(d) *CORE SIM*, thermal ($k_{\text{eff},CORE\ SIM} = 1.001498$)

Figure 2: Neutron flux normalized to the maximum flux value shown for layer 8 of 19.

The deviations between the two simulations have a smooth shape except for the amplitudes in the region around the perturbation location. At the location of the perturbation, the deviation is about $-15\,\%$, but in the adjacent node regions it is about $+10\,\%$. In regions far away from the perturbation's location, the amplitudes deviate around $+10\,\%$, and in regions of medium distance from the core center, the deviations are about 2 to $5\,\%$.

The case of the localized absorber of variable strength was investigated for various frequencies and perturbation amplitudes. As the shape functions of the induced fluctuations do not qualitatively differ from those shown in Fig. 3, only the minimum and maximum values of the deviations' absolute values are summarized in Tab. 1. It can be seen that an increase of the frequency lowers the minimum and slightly increases the maximum absolute deviation; an increase of the amplitude gives a decrease of the minimum absolute deviation and no chanche for the maximum absolute deviation.

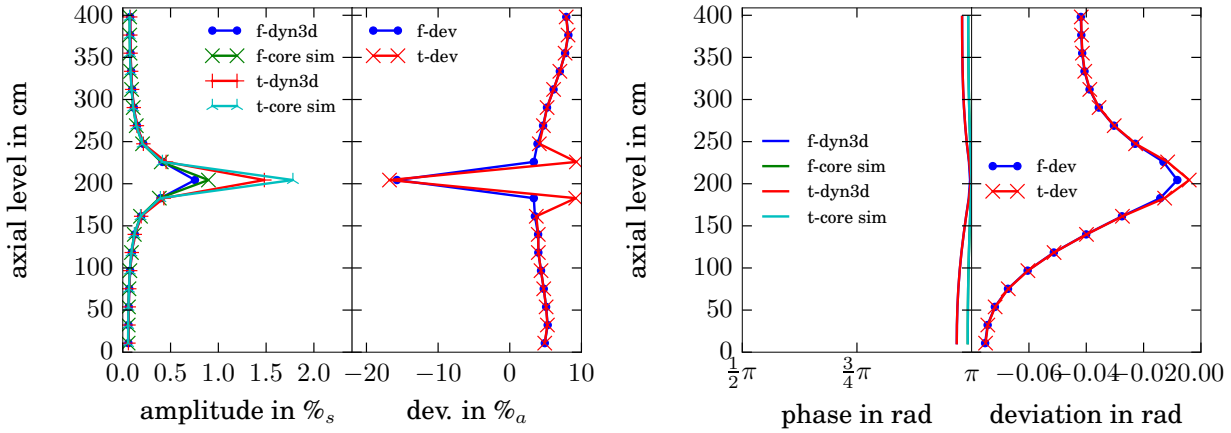

(a) Amplitude. Central channel.

(b) Phase. Central channel.

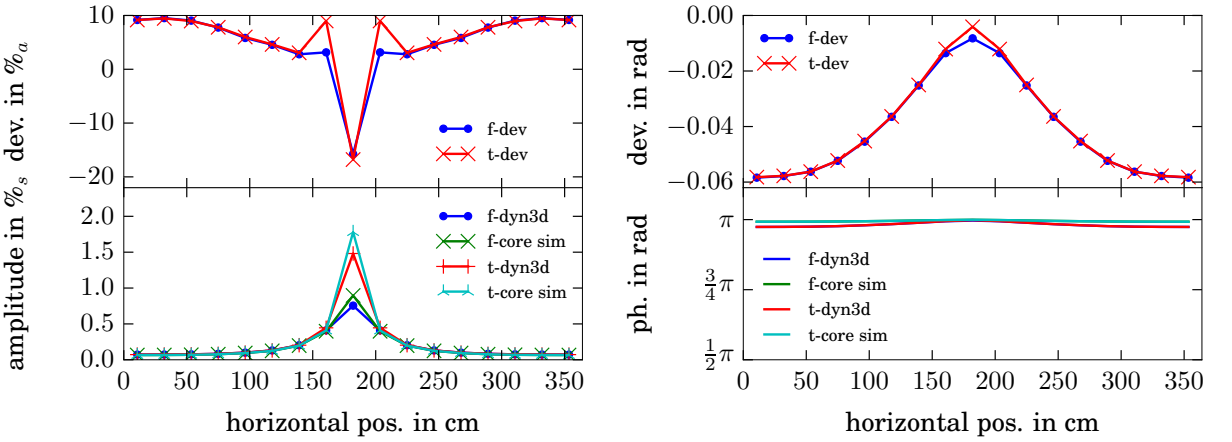

(c) Amplitude. Mid height. Central row.

(d) Phase. Mid height. Central row.

Figure 3: Neutron flux fluctuations for the fast (f) and thermal (t) energy group. Absorber of variable strength, $f = 1\,\mathrm{Hz}$, $A = 1\%\,\Sigma_{\mathrm{abs},2,0}$. Results are shown in direct comparison along with the relative deviations.

Table 1: Deviations for several parameter sets of the local absorber perturbation.

Perturbation set			Deviations (modulus)							
*): for set II cf. Fig. 3			for Amplitude in $\%_a$				for Phase in mrad			
			axial		horizontal		axial		horizontal	
No.	A_{rel} in $\%_s$	f in Hz	min	max	min	max	min	max	min	max
I)	0.5	1.0	4.00	16.7	3.56	16.7	3.61	73.1	3.61	48.2
II*)	1.0	1.0	3.70	16.8	3.06	16.8	4.08	75.1	4.08	58.2
III)	2.0	1.0	3.62	16.8	2.87	16.8	4.34	77.5	4.34	64.5
IV)	1.0	0.5	5.48	16.6	5.01	16.6	7.86	144.3	7.86	110.3
II*)	1.0	1.0	3.70	16.8	3.06	16.8	4.08	75.1	4.08	58.2
V)	1.0	2.0	2.81	16.9	2.29	16.9	1.12	20.7	1.12	14.2

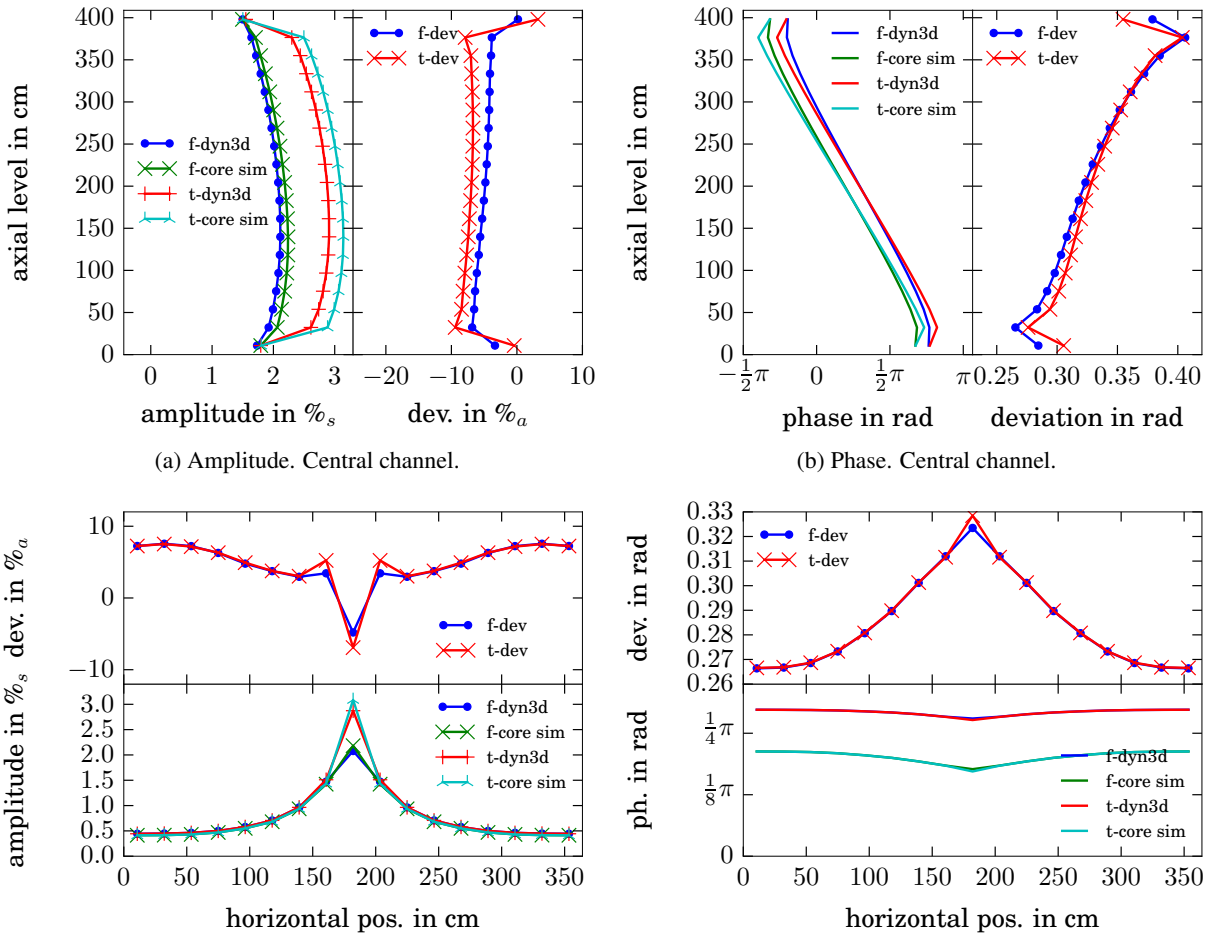

(a) Amplitude. Central channel.

(b) Phase. Central channel.

(c) Amplitude. Mid height. Central row.

(d) Phase. Mid height. Central row.

Figure 4: Neutron flux fluctuations for the fast (f) and thermal (t) energy group. Travelling absorber of variable strength, $f = 1\,\mathrm{Hz}$, $A_{\mathrm{rel}} = 1\,\%$, $v_{\mathrm{trav}} = 5\,\mathrm{m/s}$. Results are shown in direct comparison along with the relative deviations.

2.2.3. Absorber of variable strength travelling from bottom to top

Figure 4 shows the neutron flux fluctuations induced by the travelling absorber. The shapes qualitatively agree for both codes. Absolute values of the deviations are below $10\,\%$. The horizontal evaluation, cf. Figs. 4c and 4d, reveals a similar picture as with the horizontal evaluation for the localized absorber, cf. Fig. 3c and 3d, but with a comparably large (global) deviation of the phase obtained by *DYN3D* from the one obtained with *CORE SIM*.

2.3. Discussion

Using the steady-state neutron flux distributions, the comparability of the *DYN3D* model and the *CORE SIM* model was demonstrated. Deviations between the two distributions may result from the differing numerical approaches of the two codes for solving the steady-state diffusion equation.

The dynamic results showed qualitative agreement but substantial quantitative deviations. The general spatial distribution of the fluctuations can be explained as follows. (1) An increase of the thermal absorption cross section leads to a decrease of the local neutron flux. Therefore, perturbation and induced fluctuations are basically out-of-phase. (2) From the perturbation's location, the effect is transported through the reactor core and gets attenuated along its way. Therefore, the fluctuation amplitudes decrease and the phase increases with increasing distance from the location where the perturbation is applied.

The observed deviations probably result from modeling differences between *CORE SIM* and *DYN3D* and from still unharmonized numerical parameters in numerical settings in *DYN3D*. Further research is needed to fully understand and characterize the obtained differences [§], possibly including experimental data gathered in the CORTEX project [1].

It should be emphasized that the cases considered here only cover frequencies where for regions away from the perturbation, the reactor behaves essentially in a point-kinetic manner, possibly explaining the relatively good agreement of the results in these regions. At much higher frequencies, this would not be the case (cf. [14, Sec. 2.3]) and the patterns of the deviations may change.

Nevertheless, for the frequencies considered here (being most relevant for the studies on the amplitude change mentioned in the introduction) the maximum deviations are about $15\,\%$, a range that may be considered sufficiently small, in order to deduce qualitative statements about neutron-noise patterns that are induced by certain assumed perturbation sources. Thus, the paper at hand suggests that *DYN3D* may actually be used also for certain purposes of neutron-noise calculations.

3. CONCLUSIONS

Two special cases of neutron flux oscillations have been simulated with *CORE SIM* and with *DYN3D* aiming at a confirmation that the latter code may be applied for neutron noise calculations. Therefore, the source-code of *DYN3D* and the input has been adapted to provide comparable models in both codes. The latter property was justified by a comparison of the steady-state results.

The subsequent time- and frequency-dependent calculations yielded qualitatively equivalent results with quantitative deviations with magnitudes of 2 to $17\,\%$. The deviations may result from differences in the numerical approaches of the codes for solving the neutron kinetics and from an inadequate setup of some numerical parameters presumably in *DYN3D*. The deviations represent a matter of ongoing research and will be further characterized in the future.

As the maximum absolute deviations are lower than $20\,\%$, the code *DYN3D* may be considered as qualified for neutron-noise calculations.

ACKNOWLEDGEMENTS

This work was supported by the German Federal Ministry for Economic Affairs and Energy (projects DURATEA, grant number 1501490, and NEUS, grant number 1501587). The responsibility for the content of this publication lies with the authors. The research leading to these results was also partially funded from the Euratom research and training program 2014-2018 under grant agreement No 754316.

[§] Reference [10] reports about frequency-domain calculations of a 2x2 fuel assembly system performed with *CORE SIM* and a S_{16} discrete ordinates solver on a 2-dimensional domain. The relative deviations between the results are of the same order as shown here, and the maximum relative deviations seem to appear at the perturbation location as shown here, too.

REFERENCES

[1] C. Demazière, P. Vinai, M. Hursin, S. Kollias, and J. Herb. "Overview of the CORTEX project." In *PHYSOR 2018: Reactor Physics paving the way towards more efficient systems, Cancun, Mexico, April 22-26, 2018* (2018).

[2] M. Seidl, K. Kosowski, U. Schüler, and L. Belblidia. "Review of the historic neutron noise behavior in German KWU built PWRs." *Progress in Nuclear Energy*, **volume 85**, pp. 668 – 675 (2015).

[3] C. Demazière. "CORE SIM: A multi-purpose neutronic tool for research and education." *Annals of Nuclear Energy*, **volume 38**(12), pp. 2698 – 2718 (2011).

[4] K. A. T. Hoang, V.-C. Cao, V.-K. Hoang, and H.-N. Tran. "Calculation of the ex-core neutron noise induced by individual fuel assembly vibrations in two PWR cores." *Nuclear Science and Techniques*, **volume 27**(4), p. 86 (2016).

[5] U. Rohde, S. Kliem, U. Grundmann, S. Baier, Y. Bilodid, S. Duerigen, E. Fridman, A. Gommlich, A. Grahn, L. Holt, Y. Kozmenkov, and S. Mittag. "The reactor dynamics code DYN3D models, validation and applications." *Progress in Nuclear Energy*, **volume 89**, pp. 170 – 190 (2016).

[6] S. Kliem, Y. Bilodid, E. Fridman, S. Baier, A. Grahn, A. Gommlich, E. Nikitin, and U. Rohde. "The reactor dynamics code DYN3D." *Kerntechnik*, **volume 81**(2), pp. 170 – 172 (2016).

[7] M. Viebach, C. Lange, N. Bernt, M. Seidl, D. Hennig, and A. Hurtado. "PWR Neutron Noise Pattern from Coherent Fuel Assembly Deflection." In *PHYSOR 2018: Reactor Physics paving the way towards more efficient systems, Cancun, Mexico, April 22-26, 2018* (2018).

[8] N. Olmo-Juan, C. Demazière, T. Barrachina, R. Miró, and G. Verdú. "PARCS vs CORE SIM neutron noise simulations." *Progress in Nuclear Energy*, **volume 115**, pp. 169 – 180 (2019).

[9] A. Vidal-Ferràndiz, A. Carreño, D. Ginestar, C. Demazière, and G. Verdú. "NEUTRONIC SIMULATION OF FUEL ASSEMBLY VIBRATIONS IN A NUCLEAR REACTOR." In *M&C 2019: Bridging Theory and Applications, Portland, Oregon USA, August 25-29, 2019* (2019).

[10] A. Mylonakis, H. Yi, P. Vinai, and C. Demazière. "NEUTRON NOISE SIMULATIONS IN A HETEROGENEOUS SYSTEM: A COMPARISON BETWEEN A DIFFUSION-BASED AND A DISCRETE ORDINATES SOLVER." In *M&C 2019: Bridging Theory and Applications, Portland, Oregon USA, August 25-29, 2019* (2019).

[11] T. Kozlowski and T. Downar. *OECD/NEA and US NRC PWR MOX/UO2 core transient benchmark. NEA/NSC/DOC(2003) 20*. NEA Nuclear Science Committee. Working Party on Scientific Issues of Reactor Systems (2003).

[12] C. Beckert and U. Grundmann. "Development and verification of a nodal approach for solving the multigroup SP3 equations." *Annals of Nuclear Energy*, **volume 35**(1), pp. 75 – 86 (2008).

[13] C. A. Wemple, H.-N. Gheorghiu, R. Stamm'ler, and E. Villarino. "Recent Advances in the HELIOS-2 Lattice Physics Code." In *PHYSOR 2008: Nuclear Power, a Sustainable Resource, Interlaken, Switzerland, 14-19 September 2008* (2008).

[14] C. Demazière, V. Dykin, and K. Jareteg. "Development of a point-kinetic verification scheme for nuclear reactor applications." *Journal of Computational Physics*, **volume 339**, pp. 396 – 411 (2017).